J Bionic Eng 16 (2019) 954–964
DOI: https://doi.org/10.1007/s42235-019-0109-1

Multilevel Image Thresholding Using Tsallis Entropy and Cooperative Pigeon-inspired Optimization Bionic Algorithm

Yun Wang, Guangbin Zhang*, Xiaofeng Zhang

School of Physics and Information Technology, *Shaanxi Normal University*, *Xi'an* 710119, *China*

Abstract

Multilevel thresholding is a simple and effective method in numerous image segmentation applications. In this paper, we propose a new multilevel thresholding method that uses cooperative pigeon-inspired optimization algorithm with dynamic distance threshold (CPIOD) for boosting applicability and the practicality of the optimum thresholding techniques. Firstly, we employ the cooperative behavior in the map and compass operator of the pigeon-inspired optimization algorithm to overcome the "curse of dimensionality" and help the algorithm converge fast. Then, a distance threshold is added to maintain the diversity of the pigeon population and increase the vitality to avoid local optimization. Tsallis entropy is used as the objective function to evaluate the optimum thresholds for the considered gray scale images. Four benchmark images are applied to test the property and the stability of the proposed CPIOD algorithm and three other optimization algorithms in multilevel thresholding problems. Segmentation results of four optimization algorithms show that CPIOD algorithm can not only get higher quality segmentation results, but also has better stability.

Keywords: bionic algorithm, multilevel thresholding, Tsallis entropy, pigeon-inspired optimization, image segmentation

1 Introduction

Image segmentation refers to the technology and process of dividing an image into several regions with specific properties by some criteria, and then extracting the desired objects. It is a significant step towards image processing, and it is used in many fields, such as remote-sensing[1,2], bioimage informatics[3,4], and computerized examination of the industrial parts. There are various kinds of image segmentation methods[5–13], including clustering-based methods, threshold-based methods and region-based methods. Among these methods, threshold-based method is used widely in many domains because of its simplicity and ease of realization. Generally, threshold-based method is worked by minimizing or maximizing an objective function which uses the chosen thresholds as parameters. Ostu[14] and Kapur's entropy[15] are the most frequently used function to get the thresholds. However, both of them do not consider the correlations between the elements, and the accuracy of both functions is depending on the number of thresholds. In addition, the increase of threshold level will reduce the efficiency of image segmentation; so many intelligent algorithms are used to eliminate this effect, such as Particle Swarm Optimization (PSO)[16], Genetic Algorithm (GA)[17], Differential Evolution (DE)[18] and Simulate Anneal Arithmetic (SAA)[19]. Some scholars have made a lot of improvements to these optimization algorithms in order to effectively solve multilevel thresholding problems. For example, Liu *et al*. proposed an improved PSO algorithm that is applied in the field of multilevel thresholding[20]. Uros Mlakar *et al*. made substantial improvements to the DE algorithm with regard to the problem of multilevel thresholding[21].

Therefore, there are two main problems in multilevel thresholding. One is to enhance the ability of the optimization algorithm to improve the efficiency of the segmentation process, such as the multilevel thresholding method using Otsu and chaotic bat algorithm [22]. The other is to design or modify the objective function of evaluation threshold to improve the quality of the segmentation results, like, the multilevel thresholding method which uses the fuzzy entropy as the objective function[23].

Inspired by the concept of multi-fractal, Tsallis generalized standard Bolzmann-Gibbs entropy and

***Corresponding author:** Guangbin Zhang
E-mail: guangbinzhang@snnu.edu.cn

proposed the concept of Tsallis entropy[24]. Tsallis entropy has non-extensibility (Pseudo additivity) and it can describe physical systems with long-term interaction, long-term memory and fractal-type structure. There exist several studies that report the similarities among Tsallis, Shannon and Boltzmann-Gibbs entropy[25,26]. Due to the non-extensibility of Tsallis entropy, it has been applied in many fields. Image processing is one of the successful application area in numerous fields. A bi-level thresholding method which first used Tsallis entropy as the objective function is introduced in Ref. [27]. Agrawal *et al*. proposed a Tsallis entropy based optimal multilevel thresholding method using cuckoo search algorithm[28]. Diego Oliva *et al*. summarized the relevant literature in the field of multilevel thresholding and pointed out that Tsallis entropy is different from Kapur's entropy and Ostu that the Tsallis entropy produces a functional formulation whose accuracy does not depend on the number of thresholds[29]. So, in this paper, we use Tsallis entropy as the objective function to evaluate the thresholds.

In last few years, with the development of the applied mathematics and information science, various new meta-heuristic optimization algorithms have emerged, such as Brain Storm Optimization(BSO)[30], Gray Wolf Optimization(GWO)[31] and Pigeon-Inspired Optimization (PIO)[32]. These new optimization algorithms often have the characteristics of multi-structure, that is to say; they complete the tasks of exploration and exploitation respectively at different stages of the algorithm iteration. Taking PIO as an example, it converges faster and has fewer parameters than the conventional algorithm. It has been proved that PIO algorithm has advantages over conventional algorithms in standard function optimization[32]. However, it is easy to premature convergence and fall into a local optimum, and it updates the position of the particle as a whole item like PSO sufferring from the "curse of dimensionality"[33]. The performance of PIO deteriorates as the dimensionality of the search space increases. Cooperative behavior method was initially presented by Vanden *et al*.[34] to improve the performance of PSO. It decomposes a whole high-dimensional problem into several low-dimensional or one-dimensional parts. The particle in cooperative particle swarm optimization makes a contribution to the population not only as an entire item but also in each dimension.

In this study, we apply the improved pigeon-inspired optimization algorithm to multilevel thresholding. The new PIO algorithm (named cooperative pigeon-inspired optimization algorithm with dynamic distance threshold, CPIOD) could converge faster and overcome the "curse of dimensionality" with the help of the cooperative method. So, it could be helpful for improving the accuracy of optimization results and obtaining more precise threshold. Tsallis entropy is chosen as the objective function to evaluate the thresholds, so the segmentation result is more reasonable. The experimental results also confirm our hypothesis. The remainder of this paper is organized as follows. In section **2**, an overview of the PIO and the expound of CPIOD are provided and a mathematical model of the concept of Tsallis entropy is introduced. Section **3** evaluates the performance of CPIOD algorithm when it is used in multilevel thresholding by four benchmark images and section **4**, conclusion of this paper.

2 CPIOD algorithm and Tsallis entropy

2.1 PIO algorithm

Inspired by pigeon homing behavior, Duan and Qiao first proposed PIO algorithm in 2014, which was used in air robot path planning[32]. The algorithm has two main operators to imitate the pigeon's behavior, that is map and compass operator and landmark operator. Firstly, the pigeons position $\{X_{i1}, X_{i2}, \dots, X_{iM}\}$ and the velocity V_i of each pigeon are initialized in the range of the solution, where, M is the dimension of the problem to be optimized, i is the ith pigeon. In map and compass operator, pigeons in the pigeon flock rely on the "earth's magnetic field" to build a map, and use the compass to constantly correct their position and guide them to quickly approach the target. The update of its location can be described as:

$$V_i(t) = V_i(t) \cdot e^{-Rt} + rand \cdot (X_g - X_i(t-1)), \tag{1}$$

$$X_i(t) = X_i(t-1) + V_i(t-1), \tag{2}$$

where $X_i(t)$ represents the position of the current generation of pigeons, and $X_i(t-1)$ represents the position of the previous. R is the map and compass factor decided by practical problem, X_g is the global best position of all pigeons and *rand* denotes a random number in [0,1]. In map and compass operator, the pigeons are close to their destination. After that, the pigeons who are familiar with landmarks in the pigeon flock will find their destination more quickly and accurately with the help of landmarks but pigeons that are not familiar with landmarks will be abandoned. Assuming that half of the pigeons are familiar with landmarks, their center can be regarded as the target area, and it can guide them to the target faster and more accurately. The process is described below:

$$N_{\mathrm{p}}(n)=\frac{N_{\mathrm{p}}(n-1)}{2}, \tag{3}$$

$$X_{\mathrm{c}}(n)=\frac{\sum X_i(n)\cdot fitness(X_i(n))}{N_{\mathrm{p}}\cdot\sum fitness(X_i(n))}, \tag{4}$$

$$X_i(n)=X_i(n-1)+rand\cdot(X_{\mathrm{c}}(n)-X_i(n-1)), \tag{5}$$

where, X_{c} is the center of pigeons. In each iteration, the number of N_{p} (pigeon population) is halved. $fitness(X_i(n))$ is the fitness of ith pigeons in each iteration and it has different computational rules for different optimization problems. In maximizing optimization problem:

$$fitness(X_i(n))=f_{\max}(X_i(n)), \tag{6}$$

and in minimizing optimization problem:

$$fitness(X_i(n))=\frac{1}{f_{\min}(X_i(n))+e}, \tag{7}$$

where e is a small positive value that goes to 0 to prevent 0 in the denominator.

2.2 CPIOD algorithm

In map and compass operator of PIO, the pigeons in the pigeon flock keep the communication with each other by following the pigeons in the optimum position. Under the interaction of pigeons, they have the ability to achieve a new search space. Its convergence speed is fast but it is also easy to fall into local optimum, because the pigeons lack individual cognitive ability in this operator. So, in PIO algorithm, when the pigeons reach a target area quickly with the help of "map and compass", the algorithm switches to landmark operator to help pigeons reach their destination more accurately. Therefore, in map and compass operator, the closer the pigeon group arrives to the target, the better the final result will be. Like many other swarm optimization algorithms, PIO algorithm also suffers from "curse of dimensionality". In map and compass operator, with the increase of the dimension of the problem, the global search ability of particles will decrease. So, a cooperative mechanism is introduced in the new algorithm to mitigate this effect. In a n-dimensional optimization problem, each pigeon in the pigeon flock represents a potential solution. In the process of location updating, some dimensions of the pigeons are modified to be closer to the target, but some dimensions may leave the original better position. In Van Den Bergh's paper[34], this phenomenon is called "two steps forward one step back". To solve this problem, the idea that each dimension of the n-dimensional problem can be updated separately produces a cooperative approach which initializes n subgroups to optimize different dimensions.

In map and compass operator, the pigeons in the flock follow the pigeons in the best position X_{g}. In order to keep the algorithm from stagnating in the early stages, pigeons need to keep a certain distance ($d=\|X_i-X_{\mathrm{g}}\|^2$) from X_{g}. Once the distance between them is too close ($d<D$) and the corresponding velocity is less than a certain value, the position of the pigeon will be reset. D is called distance threshold. As you can see in Fig. 1, the distance between X_3 and X_{g} is less than D, so X_3 will be reset in the solution space. The goal of setting such a threshold is to prevent the flock from gathering prematurely and thus inactivating the flock.

However, with the gradual convergence of the algorithm, if the pigeons always keep such distance from X_{g}, it is not conducive to the local exploitation of the algorithm in the later stage. So in the latter part of the algorithm, it only needs a small distance to keep the algorithm active. That is to say, it is hoped that the value

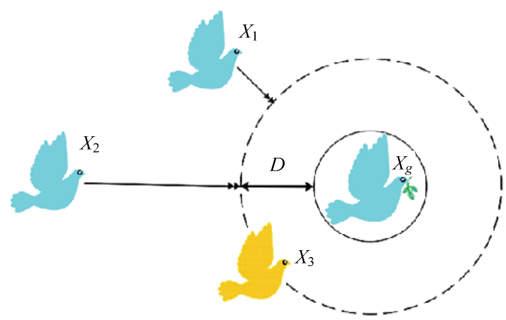

Fig. 1 Pigeons optimization model.

of D will gradually decrease with the iteration, which can be expressed as:

$$D = w \cdot D_c, \tag{8}$$

where, D_c is the initial value, w is the threshold factor,

$$w = 1 - t / iter, \tag{9}$$

where, t is the tth iteration and $iter$ is the numbers of iteration. So as the algorithm iterates, pigeons gradually change from searching in the whole space to searching locally.

2.3 Multilevel thresholding using Tsallis entropy

Tsallis entropy is widely used in multiple image processing applications such as biomedical analysis and automatic target recognition. It introduces parameter q to measure the non-extensibility of the system which could be express as:

$$S_q = \frac{1 - \sum_{i=1}^{k} (p_i)^q}{q - 1}, \tag{10}$$

where, p_i represents the probability of finding the system in each possible state i , thus $0 \le p_i \le 1$ and $\sum_i^k p_i = 1$, k denotes the total number of states. Based on pseudo-additivity, the Tsallis entropy of the system can be expressed as

$$S_q(A + B) = S_q(A) + S_q(B) + (1 - q) S_q(A) S_q(B). \tag{11}$$

In image segmentation, the gray level range of the input image pixels is $\{1,2,\ldots,G\}$, p_i represents the probability of each gray level pixel in the total pixel. In single-level threshold, pixels are classified by threshold t_1 into two classes, which are object of interest (O) and background (B). Based on the above definition, the entropy formula can be given:

$$S_q(O) = \frac{1 - \sum_{i=1}^{t_1} (p_i / p_O)^q}{q - 1} \quad \text{and}$$

$$S_q(B) = \frac{1 - \sum_{i=t_1+1}^{G} (p_i / p_B)^q}{q - 1}. \tag{12}$$

where, $p_O = \sum_{i=1}^{t_1} p_i$, $p_B = \sum_{i=t_1+1}^{G} p_i$ and $p_O + p_B = 1$.

The threshold corresponding to the maximum amount of information between the object and the background is the optimal segmentation threshold:

$$T_{\text{opt}} = \arg\max[S_q(O) + S_q(B) + (1 - q) \cdot S_q(O) \cdot S_q(B)]. \tag{13}$$

On this basis, it can be easily extended to multi-level thresholding:

$$[T_1, T_2, \ldots T_m] = \arg[S_q(1) + S_q(2) + \ldots + S_q(m+1) + (1 - q) \cdot S_q(1) \cdot S_q(2) \ldots S_q(m+1)] \tag{14}$$

where,

$$S_q(1) = \frac{1 - \sum_{i=1}^{t_1} (\frac{p_i}{p_1})^q}{q - 1}, \quad S_q(2) = \frac{1 - \sum_{i=t_1+1}^{t_2} (\frac{p_i}{p_2})^q}{q - 1}, \ldots, \quad S_q(m+1) = \frac{1 - \sum_{i=t_m+1}^{G} (\frac{p_i}{p_{m+1}})^q}{q - 1}. \tag{15}$$

$p_1, p_2, \ldots, p_{m+1}$ is the probability distribution of $m + 1$ classes with m thresholds.

The improved CPIOD algorithm and Tsallis entropy multilevel thresholding method are combined to find the best threshold for image segmentation. The algorithm can be described by the following steps, and Fig. 2 shows the flow chart of CPIOD.

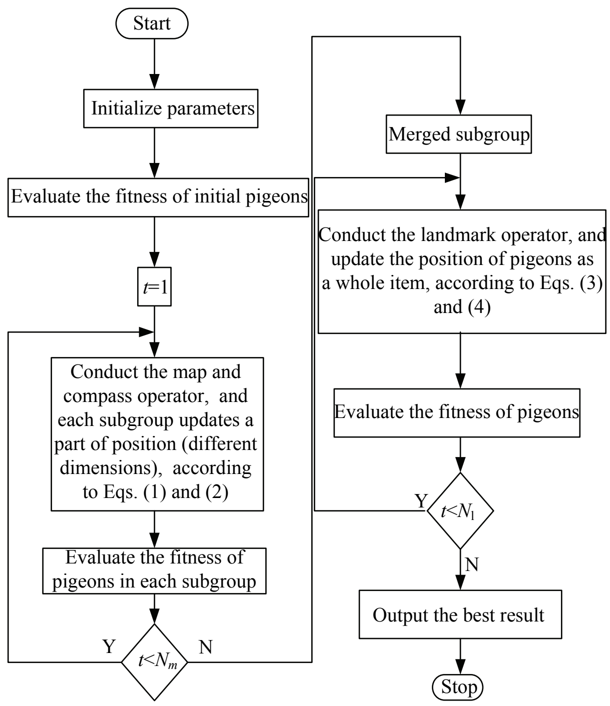

Fig. 2 The flow chart of CPIOD algorithm.

Step1 Initialize parameters of CPIOD and randomly generate pigeon positions in the solution space.

Step2 Evaluate the fitness of pigeons in different subgroups and find the pigeon with the best position in the initial pigeons of each subgroup. Combine the optimal solution of (M/K)-dimension of each subgroup into a global optimal solution (X_g) of D-dimension.

Step3 Conduct map and compass operations. Each subgroup updates the different dimensions of the solution. Evaluate the fitness values and update X_g according Eqs. (1) and (2).

Step4 Merge the subgroups after N_m iterations to continue the landmark operator. Update the position of the fused population as a whole item.

Step5 Evaluate the fitness of pigeons and update the position of X_g according to Eqs. (4) and (5) until the termination condition is satisfied. Then, output the best result.

3 The performance and quantitative evaluation of CPIOD

The performance of the proposed CPIOD is evaluated by comparing its results with original PIO algorithm, GWO algorithm and PSO algorithm. These algorithms are implemented in MATLAB 2014a and the hardware configuration is Intel core i5 8500 3.0GHz CPU with 16G memory, running windows 10. Four benchmark images (Airfield, couple, loco, peppers) are used for testing the performance of the algorithms. Fig. 3 shows these images and their corresponding histograms.

The performance of algorithms is closely related to their parameter selection. In general, it is unlikely to identify the optimal set of such parameters. Therefore, the parameters need to be tested before the simulation. We choose the parameters that provide the best computational results in the light of the best thresholds and corresponding computational stability. The selected parameters are listed in Table 1.

In our simulation, each algorithm runs 50 times to guarantee the availability of the obtained result. The average objective function values of these algorithms in 50 runs and the thresholds corresponding to the optimal objective function values obtained by each algorithm in 50 runs will be compared. Table 2 shows the mean of the objective function values (Ob) and the optimal threshold values (Th) obtained using CPIOD, GWO, PSO, and PIO, in which m is the number of thresholds.

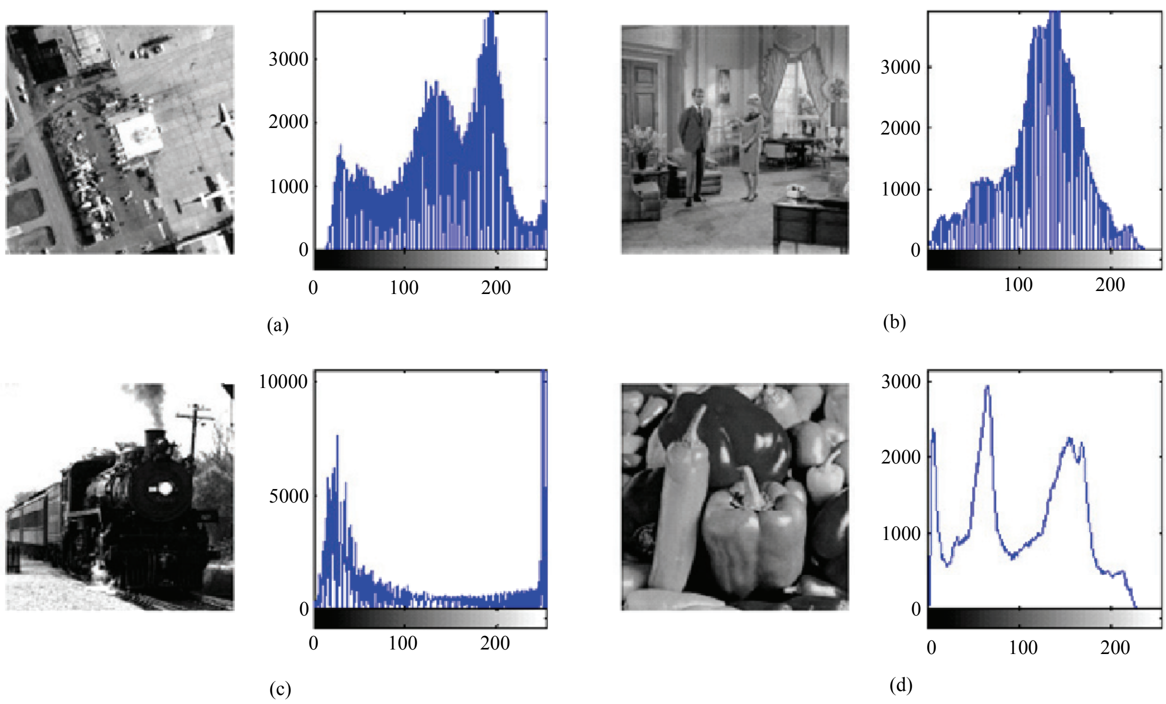

Fig. 3 Test images and their corresponding histograms: (a) Airfield, (b) couple, (c) loco and (d) peppers.

Table 1 Parameters used for CPIOD, PIOD, PIOS and PIO

Parameters	CPIOD	GWO	PSO	PIO
Total iteration number (N)	50	50	50	50
Number of iterations for map and compass operations (N_m)	45	~	~	45
Iteration number of landmark operations (N_l)	5	~	~	5
Initial value of distance and velocity threshold (D,V)	(10,0.1)	~	~	(20,0.1)
Map and compass factor (R)	0.1	~	~	0.1
Population size (P)	20	20	~	20
Number of subgroups (K)	2	~	~	~
Acceleration coefficient (C_1,C_2)	~	~	2	~
Inertia weighting coefficient ($W_{\max}$, $W_{\min}$)	~	~	(0.9,0.4)	~

Table 2 Mean objective function values and optimal threshold values

Image	m	CPIOD		GWO		PSO		PIO	
		Ob	*Th*	*Ob*	*Th*	*Ob*	*Th*	*Ob*	*Th*
Airfield	2	**21.0123**	98,168	21.0122	98,168	20.9746	98,168	21.0065	98,168
	3	**39.8827**	71,121,178	39.8810	71,121,178	39.5563	71,121,178	39.7764	71,121,178
	4	**88.2767**	66 109,154,200	88.2274	66 109,154,199	86.3200	66 109,154,200	86.3943	64 108,154,199
	5	**208.2860**	60,98, 134,170,205	207.4945	60,97 134,169,205	199.0867	57,96 133,169,205	199.3168	60,94 133,166,205
Couple	2	**21.9128**	94,173	21.9125	94,173	21.8843	94,173	21.9046	94,173
	3	**44.0020**	55,107,175	43.9963	55,107,175	43.7336	55,107,175	43.8164	55,107,175
	4	**105.0328**	50 98,144,190	104.9824	50 98,144,190	102.4162	50 98,144,190	103.5033	50 98,146,190
	5	**269.2273**	47,88 126,164,199	268.4048	47,88 126,164,199	258.3391	47,88 126,164,199	255.4591	47,89 125,165,200
Loco	2	**15.9933**	73,142	15.9951	73,142	15.9682	73,142	15.9897	73,142
	3	**28.9041**	64,121,170	28.8883	64,121,170	28.6116	64,121,170	28.7563	64,121,170
	4	**59.0797**	54 102,143,184	58.9938	57 102,140,184	57.7205	57 102,143,184	58.1294	57 105,143,184
	5	**134.2749**	45,83 121,153,193	133.3493	45,83 121,154,193	128.0623	45,83 120,156,195	128.2857	45,84 122,154,193
Peppers	2	**24.3964**	97,176	**24.3964**	97,176	24.3306	97,176	24.3497	97,176
	3	54.6572	72,125,177	**54.8065**	72,125,177	54.2351	72,125,177	54.3819	72,125,177
	4	**141.6017**	47 86,130,178	141.5384	47 86,130,178	136.6394	47 86,130,178	137.7403	47 86,130,178
	5	**395.4447**	45,76 110,144,180	394.8523	45,76 110,143,180	177.1618	45,76 110,144,180	372.8457	47,76 112,146,181

From Table 2, it is obvious that CPIOD algorithm exceeds the other algorithms in the light of obtaining the maximum of the objective function values of these images. The bold numbers in the table represent the maximum function values that can be obtained by each algorithm under the same number of thresholds. In most cases, CPIOD has shown its superiority, although the performance of CPIOD is not outstanding when the number of thresholds is small. It is also shown that the introduction of cooperative mechanism helps PIO algorithm to improve the optimization ability for the high-dimensional functions. With the increase of the threshold number, the advantage of CPIOD algorithm is highlighted.

The segmentation results for CPIOD, GWO, PSO, and PIO are shown in Figs. 4 and 5 (with two and five threshold) to evaluate the performance of the proposed CPIOD algorithm in image segmentation. From a visualization perspective, the results of the segmentation verify the above conclusions from Table 2. For example, airfield is a gray-scale image, which is shown in Fig. 3. When the threshold number is 2, there is no significant difference between the segmentation results of the different algorithms. Whereas, in Fig. 4, when the threshold number is 5, it is easy to distinguish the ground, aircraft and buildings from the result obtained by CPIOD while these objects are all mixed up in the result of PIO. The advantages of CPIOD algorithm in the case of the great number of threshold are intuitively reflected.

To quantify the differences between different methods we use, we further evaluate the peak signal-to-noise ratio (PSNR) and the structural similarity index (SSIM) of the segmentation results which are often used to estimate the image quality. PSNR is an objective indicator, the higher the PSNR value, the closer the segmented image to the original image. SSIM is related to the lightness and structure which evaluate the visual likeness between original image and segmented image; it can reflect the subjective perception of human eyes. Higher values of the PSNR and SSIM indicate the better segmentation results. The mathematical expressions for choosing constraints (metrics) are introduced in Refs. [35] and [36].

Table 3 and Table 4 record the mean and standard deviation (std) values of PSNR and SSIM of the segmented images after 50 runs of these algorithms. Compared to the other algorithms, it can be noted that the proposed CPIOD algorithm has the superior metric values in the case of different threshold numbers. Especially, when the threshold number is 4 or 5, the superiority of CPIOD algorithm is particularly obvious. Because the additional relevant information extracted by the CPIOD algorithm is more than that of other algorithms, and the extraction of noise pixels is also more. So the PSNR value is higher in some cases. The SSIM metric is also related to the noise pixels of the image and can provide better similarity index values. Therefore, in those algorithms considered in this paper, CPIOD algorithm provides better output through the use of multilevel thresholding method to extract information from images.

Fig. 4 The result of image segmentation with two thresholds.

Fig. 5 The result of image segmentation with five thresholds.

Table 3 Mean and std values of PSNR

Image	m	CPIOD		GWO		PSO		PIO	
		Mean	std	Mean	std	Mean	std	Mean	std
Airfield	2	**14.3602**	0	14.3576	1.31E−02	14.2835	3.10E−01	14.3071	1.38E−01
	3	**16.3930**	1.43E−14	16.3385	6.60E−02	16.2995	1.06E−00	16.2050	4.50E−01
	4	20.2987	3.33E−02	**20.3837**	2.60E−01	19.9874	1.16E−00	19.2654	1.49E−00
	5	21.8841	1.61E−03	22.1905	2.87E−01	**22.2126**	8.59E−01	21.1287	1.23E−01
Couple	2	**16.0511**	5.63E−04	16.0343	5.87E−02	15.9570	3.75E−01	16.0032	1.95E−01
	3	**19.4480**	6.28E−02	19.4144	9.39E−02	19.2606	3.75E−01	19.2636	3.24E−01
	4	**22.5542**	9.48E−02	22.4073	1.99E−01	22.4685	5.20E−01	21.7101	9.23E−01
	5	**24.6654**	7.96E−02	24.6512	1.94E−01	24.3317	5.60E−01	23.5373	1.56E−00
Loco	2	**17.5207**	5.33E−03	17.4439	6.92E−03	17.3753	2.60E−01	17.4508	1.07E−01
	3	**19.6326**	2.15E−14	19.5828	6.76E−02	19.5866	3.90E−01	19.5420	2.89E−01
	4	**20.9691**	1.23E−01	20.9313	1.43E−01	20.9245	4.69E−01	20.7256	4.70E−01
	5	**22.3256**	1.21E−03	22.1488	1,88E−01	22.2900	6.38E−01	21.6804	6.25E−01
Peppers	2	**15.1644**	1.81E−03	15.1642	1.25E−02	15.0729	7.72E−01	14.6293	1.29E−00
	3	17.1176	6.51E−01	16.9736	5.18E−02	**17.2386**	8.91E−01	16.9745	5.36E−01
	4	**21.0936**	3.22E−02	21.0032	1.11E−01	20.7132	1.45E−00	19.5497	1.91E−00
	5	21.9958	5.07E−02	22.1411	1.72E−01	**22.4508**	9.36E−01	21.5140	1.54E−01

Table 4 Mean and std values of SSIM

Image	m	CPIOD		GWO		PSO		PIO	
		Mean	std	Mean	std	Mean	std	Mean	std
Airfield	2	**0.4686**	3.36E−16	**0.4686**	6.14E−04	0.4668	1.13E−02	0.4684	6.80E−03
	3	**0.5470**	3.36E−16	**0.5470**	1.61E−03	0.5419	1.12E−02	0.5410	7.81E−03
	4	0.6108	3.28E−04	**0.6125**	3.71E−03	**0.6125**	1.31E−02	0.6064	9.71E−03
	5	0.6785	2.81E−04	**0.6816**	4.81E−03	0.6789	1.51E−02	0.6638	2.03E−02
Couple	2	**0.4730**	1.36E−05	0.4727	8.48E−04	0.4707	1.13E−02	0.4721	3.15E−03
	3	**0.5993**	1.11E−04	**0.5993**	3.98E−04	0.5911	1.44E−02	0.5888	1.27E−02
	4	**0.6790**	2.10E−03	0.6773	2.43E−03	0.6698	1.18E−02	0.6617	1.60E−02
	5	**0.7281**	1.41E−03	0.7263	3.53E−03	0.7122	1.62E−02	0.7085	1.97E−02
Loco	2	0.4778	3.30E−02	**0.4795**	4.31E−02	0.4779	7.43E−02	0.4782	4.65E−02
	3	**0.5424**	4.49E−16	0.5411	1.90E−03	0.5413	1.19E−02	0.5411	8.41E−03
	4	0.5901	4.21E−03	0.5885	4.63E−03	0.5900	1.56E−02	0.5843	1.66E−02
	5	**0.6402**	6.84E−05	0.6326	7.51E−03	0.6375	2.50E−02	0.6171	2.16E−02
Peppers	2	**0.3681**	4.37E−05	0.3546	5.90E−04	**0.3681**	1.08E−02	0.3634	6.31E−03
	3	0.4389	3.26E−02	0.4315	1.91E−03	**0.4413**	3.49E−02	0.4345	2.51E−02
	4	**0.6141**	1.51E−03	0.6115	4.11E−03	0.5833	6.00E−02	0.5558	6.71E−00
	5	0.6429	8.05E−04	**0.6450**	3.91E−03	0.6381	2.38E−02	0.6125	4.33E−02

Besides, the stability of these algorithms is evaluated by the standard deviation (std) of the results. A lower value of std indicates the lower differences between the results obtained by the algorithm, which means the higher stability of the algorithm. The std values of PSNR and SSIM that using CPIOD vary from 0 to 6.51E−01 and 3.36E−16 to 3.30E−02, while other algorithms vary from 1.31E−02 to 1.91E−00 and 6.14E−04 to 4.31E−02. We can obtain the stability order of the algorithm from the Tables 3 and 4, that is: CPIOD > GWO > PIO > PSO. It means CIPOD algorithm can not only get better results but also has better stability compared with other algorithms. In addition, we find that although the CPIOD algorithm is not much different from the PSO algorithm in image segmentation results, its stability is better than that of the PSO algorithm, which also shows that the introduction of dynamic distance threshold improves the stability of the algorithm.

4 Conclusion

In this work, an improved PIO algorithm is used for image segmentation. The application of the cooperative mechanism improves the optimization ability of the algorithm when the number of threshold is great. In addition, the introduction of dynamic distance threshold can help the algorithm balance its global exploration ability and local exploitation ability in map and compass operator. The segmentation results of four different kinds of images confirm that the proposed CPIOD algorithm offers superior image quality measurement values compared to its original PIO algorithm and other modified algorithms. Our future work is to apply the CPIOD algorithm to different image segmentation methods and extend it to many other aspects of image processing.

Acknowledgment

This work was supported by the National Natural Science Foundation of China (Grant Nos. 11574191 and 11674208).

References

[1] Bhandari A K, Kumar A, Singh G K. Tsallis entropy based multilevel thresholding for colored satellite image segmentation using evolutionary algorithms. *Expert Systems with Applications*, 2015, **42**, 8707–8730.

[2] Bhandari A K, Kumar A, Singh G K. Modified artificial bee colony based computationally efficient multilevel thresholding for satellite image segmentation using Kapur's, Otsu and Tsallis functions. *Expert Systems with Applications*, 2015, **42**, 1573–1601.

[3] Manickavasagam K, Sutha S, Kamalanand K. An automated system based on 2d empirical mode decomposition and

k-means clustering for classification of Plasmodium species in thin blood smear images. *BMC Infectious Diseases*, 2014, **14**, 13.

[4] Manickavasagam K, Sutha S, Kamalanand K. Development of systems for classification of different plasmodium species in thin blood smear microscopic images. *Journal of Advanced Microscopy Research*, 2014, **9**, 86–92.

[5] Cuevas E, Sossa H. A comparison of nature inspired algorithms for multi-threshold image segmentation. *Expert Systems with Applications*, 2013, **40**, 1213–1219.

[6] Huang L, He D, Yang S X. Segmentation on ripe Fuji apple with fuzzy 2D entropy based on 2D histogram and GA optimization. *Intelligent Automation* & *Soft Computing*, 2013, **19**, 239–251.

[7] Caponetti L, Castellano G, Basile M T, and Corsini V. Fuzzy mathematical morphology for biological image segmentation. *Applied Intelligence*, 2014, **41**, 117–127.

[8] Han X H, Xiong X, Duan F. A new method for image segmentation based on BP neural network and gravitational search algorithm enhanced by cat chaotic mapping. *Applied Intelligence*, 2015, **43**, 855–873.

[9] Castellano G, Fanelli A M, Torsello M A. Shape annotation by semi-supervised fuzzy clustering. *Information Sciences*, 2014, **289**, 148–161.

[10] Ramík D M, Sabourin C, Moreno R, Madani K. A machine learning based intelligent vision system for autonomous object detection and recognition. *Applied Intelligence*, 2014, **40**, 358–375.

[11] Nakib A, Oulhadj H, Siarry P. Image thresholding based on Pareto multiobjective optimization. *Engineering Applications of Artificial Intelligence*, 2010, **23**, 313–320.

[12] Peng B, Zhang L, Zhang D. A survey of graph theoretical approaches to image segmentation. *Pattern Recognition*, 2013, **46**, 1020–1038.

[13] Brink A D. Minimum spatial entropy threshold selection. *IEEE Proceedings-Vision*, *Image and Signal Processing*, 1995, **142**, 128–132.

[14] Goh T Y, Basah S N, Yazid H, Safar M J A, Saad F S A. Performance analysis of image thresholding: Otsu technique. *Measurement*, 2018, **114**, 298–307.

[15] Kapur J N, Sahoo P K, Wong A K C. A new method for gray-level picture thresholding using the entropy of the histogram. *Computer Vision*, *Graphics*, *and Image Processing*, 1985, **29**, 273–285.

[16] Eberhart R, Kennedy J. A new optimizer using particle swarm theory. *MHS'95*. *Proceedings of the Sixth International Symposium on Micro Machine and Human Science*, Nagoya, Japan, 1995, 39–43.

[17] Whitley D. A genetic algorithm tutorial. *Statistics and Computing*, 1994, **4**, 65–85.

[18] Storn R, Price K. Differential evolution–a simple and efficient heuristic for global optimization over continuous spaces. *Journal of Global Optimization*, 1997, **11**, 341–359.

[19] Kirkpatrick S, Gelatt C D, Vecchi M P. Optimization by simulated annealing. *Science*, 1983, **220**, 671–680.

[20] Liu Y, Mu C, Kou W, Liu J. Modified particle swarm optimization-based multilevel thresholding for image segmentation. *Soft Computing*, 2015, **19**, 1311–1327.

[21] Mlakar U, Potočnik B, Brest J. A hybrid differential evolution for optimal multilevel image thresholding. *Expert Systems with Applications*, 2016, **65**, 221–232.

[22] Satapathy S C, Raja N S M, Rajinikanth V, Ashour A S, Dey N. Multi-level image thresholding using Otsu and chaotic bat algorithm. *Neural Computing and Applications*, 2018, **29**, 1285–1307.

[23] Naidu M S R, Kumar P R, Chiranjeevi K. Shannon and fuzzy entropy based evolutionary image thresholding for image segmentation. *Alexandria Engineering Journal*, 2018, **57**, 1643–1655.

[24] Tsallis C. Possible generalization of Boltzmann-Gibbs statistics. *Journal of Statistical Physics*, 1988, **52** 479–487.

[25] Tsallis C. Entropic nonextensivity: A possible measure of complexity. *Chaos*, *Solitons* & *Fractals*, 2002, **13**, 371–391.

[26] Zhang Y, Wu L. Optimal multi-level thresholding based on maximum Tsallis entropy via an artificial bee colony approach. *Entropy*, 2011, **13**, 841–859.

[27] De Albuquerque M P, Esquef I A, Mello A R G. Image thresholding using Tsallis entropy. *Pattern Recognition Letters*, 2004, **25**, 1059–1065.

[28] Agrawal S, Panda R, Bhuyan S, Panigrahi B K. Tsallis entropy based optimal multilevel thresholding using cuckoo search algorithm. *Swarm and Evolutionary Computation*, 2013, **11**, 16–30.

[29] Oliva D, Elaziz M A, Hinojosa S. *Metaheuristic Algorithms for Image Segmentation*: *Theory and Applications*, Springer-Verlag, Berlin, Germany, 2019.

[30] Shi Y. Brain storm optimization algorithm. *IEEE Congress on Evolution Computation*, Neworleans, USA, 2011, 1–14.

[31] Mirjalili S, Mirjalili S M, Lewis A. Grey wolf optimizer. *Advances in Engineering Software*, 2014, **69**, 46–61.

[32] Duan H, Qiao P. Pigeon-inspired optimization: A new swarm intelligence optimizer for air robot path planning. *International Journal of Intelligent Computing and Cybernetics*, 2014, **7**, 24–37.

[33] Gao H, Xu W, Sun J, Tang Y. Multilevel thresholding for image segmentation through an improved quantum-behaved particle swarm algorithm. *IEEE Transactions on Instrumentation and Measurement*, 2009, **59**, 934–946.

[34] Van den Bergh F, Engelbrecht A P. A cooperative approach to particle swarm optimization. *IEEE Transactions on Evolutionary Computation*, 2004, **8**, 225–239.

[35] Wang Z, Bovik A C, Sheikh H R, Simoncelli E P. Image quality assessment: From error measurement to structural similarity. *IEEE Transactions on Image Processing*, 2004, **13**, 600–613.

[36] Hore A, Ziou D. Image quality metrics: PSNR vs. SSIM. 2010 20*th International Conference on Pattern Recognition*, Istanbul, Turkey, 2010, 2366–2369.